Heliyon 10 (2024) e39330

Contents lists available at ScienceDirect

Heliyon

journal homepage: www.cell.com/heliyon

Research article

Analyzing the dynamics of COVID-19 transmission in select regions of the Philippines: A modeling approach to assess the impact of various tiers of community quarantines

May Anne E. Mata [a,b,c,d,*,1], Rey Audie S. Escosio [d,e,f,g,1], El Veena Grace A. Rosero [b,c,2], Jhunas Paul T. Viernes [h,2], Loreniel E. Anonuevo [a,i,j], Bryan S. Hernandez [e], Joel M. Addawe [d,h], Rizavel C. Addawe [d,h], Carlene P.C. Pilar-Arceo [d,e], Victoria May P. Mendoza [d,e], Aurelio A. de los Reyes V [a,d,e]

[a] *Mindanao Center for Disease Watch and Analytics (DiWA), University of the Philippines Mindanao, Tugbok District, Davao City, 8000, Philippines*
[b] *Interdisciplinary Applied Modeling (IAM) Laboratory, University of the Philippines Mindanao, Tugbok District, Davao City, 8000, Philippines*
[c] *Department of Mathematics, Physics, and Computer Science, University of the Philippines Mindanao, Tugbok District, Davao City, 8000, Philippines*
[d] *University of the Philippines Resilience Institute, University of the Philippines Diliman, Quezon City, 1101, Philippines*
[e] *Institute of Mathematics, University of the Philippines Diliman, Quezon City, 1101, Philippines*
[f] *Faculdade de Ciências, Universidade de Lisboa, Lisbon, 1749-016, Portugal*
[g] *BioISI—Biosystems & Integrative Sciences Institute, Faculdade de Ciências, Universidade de Lisboa, Lisbon, 1749-016, Portugal*
[h] *Department of Mathematics and Computer Science, University of the Philippines Baguio, Baguio City, 2600, Philippines*
[i] *Mapúa Malayan Colleges Mindanao, Davao City, 8000, Philippines*
[j] *Mathematics Department, Caraga State University, Ampayon, Butuan City, 8600, Philippines*

ARTICLE INFO

Keywords:
Community quarantine
Compartmental model
Coronavirus
Population factor
SEIR
Time-varying reproduction number

ABSTRACT

The COVID-19 pandemic has significantly impacted communities worldwide, and effective management strategies are critical to reduce transmission rates and minimize the impact of the disease. In this study, we modeled and analyzed the COVID-19 transmission dynamics and derived relevant epidemiological values for three regions of the Philippines, namely, the National Capital Region (NCR), Davao City, and Baguio City, under different community quarantine implementations. The unique features and differences of these regions-of-interest were accounted for in simulating the disease spread and in estimating key epidemiological parameters fitted to the reported COVID-19 cases. Results support the robustness of the model formulated and provides insights into the effect of the government's implemented intervention protocols. With a forecasting feature, this modeling framework is beneficial for science-based decision support, policy making, and assessment for recent and future pandemics wherever regions-of-interest.

* Corresponding author at: Mindanao Center for Disease Watch and Analytics (DiWA), University of the Philippines Mindanao, Tugbok District, Davao City, 8000, Philippines.
E-mail address: memata@up.edu.ph (M.A.E. Mata).
[1] These authors have equal first authorship credits.
[2] These authors have equal contributions.

https://doi.org/10.1016/j.heliyon.2024.e39330
Received 2 April 2024; Received in revised form 11 October 2024; Accepted 11 October 2024

Available online 17 October 2024

1. Introduction

Coronavirus Disease 2019 (COVID-19) is an infectious disease caused by the novel coronavirus SARS-CoV-2 and is mainly characterized by flu-like symptoms, loss of taste or smell, and respiratory problems, etc. [1]. The earliest outbreak of the disease was observed in December 2019, in Wuhan, China and had since quickly spread across different countries, resulting in a great number of fatalities [2]. On March 11, 2020, the World Health Organization officially declared it as pandemic [3].

The first and second COVID-19 patients in the Philippines were confirmed on January 30, 2020. They were tourists from mainland China who had traveled to Wuhan City [4]. A month later, several cases were discovered, both with and without travel history abroad. This was followed by the continuous rise of COVID-19 cases in the country [5].

The Philippine government enforced measures to control the disease, among which involved the implementation of community quarantines. Based on the guidelines provided by the *Philippine Inter-Agency Task Force for the Management of Emerging Infectious Diseases* (IATF-EID), community quarantines involve temporary lockdowns of an area or region entailing the presence of uniformed personnel to enforce protocol [6]. This intervention aims to mitigate the spread of the disease by limiting the movement of people [7]. However, certain groups of people were exempted from this, such as medical workers, uniformed personnel, emergency responders, manufacturers, and couriers [8]. Generally, while a community quarantine was in effect, a curfew was imposed and mass gatherings were prohibited. Traveling between cities or municipalities was restricted. Businesses and organizations that provide non-essential services were closed while operating vital services were required to follow the minimum health protocol, which included the observance of social distancing, wearing of masks and face shields, constant disinfection, and so on [9].

The IATF-EID classified quarantine periods into the following classifications: Enhanced Community Quarantine (ECQ), Modified Enhanced Community Quarantine (MECQ), General Community Quarantine (GCQ), and Modified General Community Quarantine (MGCQ). During ECQ and MECQ, only essential workers and designated household representatives were allowed outside of their residences. These designated household representatives were those identified as the member of each household responsible for obtaining provisions for their families. Although both quarantine periods enforced strict monitoring and control of the population's movement, MECQ permitted a much less stringent management as it was a phase for transitioning into GCQ.

During GCQ and MGCQ, some non-essential workers under certain age groups were allowed outside of their residences. Nevertheless, both quarantine periods were still subject to moderate regulation. During MGCQ, however, measures were more relaxed as it served as a phase for transitioning into the New Normal – the new state or situation where there is a fundamental shift in the nature/behavior of organizations and citizens in response to the new social, health, and economic realities in a mid-post-COVID-19 world [6,10].

The severity of local COVID-19 situation was the primary basis in deciding which quarantine period was to be implemented [11]. However, the IATF-EID's protocols on such quarantine period may be amended by the local government unit (LGU) depending on the needs and circumstances of each respective province, municipality, or city. These modifications were necessary as Philippines is characterized by a range of different factors unique to the respective LGUs including but not limited to topographical, climatic, socio-cultural, and demographical differences [12–14]. There were also apparent differences in available resources like manpower, hospitals, and fund allocation which varied from LGU to LGU vastly affecting the measures an LGU can impose and the extent of which it can sustain and implement such initiative [15,11]. It is apparent that the efficacy of the intervention protocols and the severity of the spread of the pathogen were affected by different factors unique to a region. However, this insight remains to be tested especially in the context of the Philippines, an archipelagic country.

Epidemiological models played a pivotal role in providing deeper understanding on how the many interconnected factors affect COVID-19 transmission [16]. Among the epidemiological models widely used and studied in this context were the SIR (Susceptible-Infected-Recovered), SEIR (Susceptible-Exposed-Infected-Recovered), and SUIR (Susceptible-Unidentified-Identified-Recovered) models [17–19]. Recent mathematical models of COVID-19 incorporate time-dependent parameters to capture multiple phases influenced by public health interventions and viral variants [20], changing contact patterns [21], demographic shifts [22], and comorbidities such as diabetes [23]. They also account for time delays to reflect intervention and medical resource availability [24] and model higher-order interactions through networks to represent non-pharmaceutical interventions [25,26]. Other recent studies focus on in-host dynamics of SARS-CoV-2 [27], estimating human mobility rates and their implications for understanding COVID-19 dynamics [28], and estimating the time-dependent effective reproduction number [29]. With the many complexities involved in epidemics, we needed a model that would be able to mathematically describe the spread of the virus, provide a tractable analysis on the effect of interventions, and simulate projections on the probable growth or decline of infections. The model should also have an innate flexibility that could account for diverse factors affecting different aspects of the disease transmission dynamics; such factor including the circumstantial differences among LGUs in the Philippines [30,31]. Hence, to illustrate the regional dynamics of COVID-19 in the Philippines and to capture the effect of the efforts to mitigate the pandemic, we developed a modified SEIR compartmental model and verified whether the model could capture the virus transmission at the selected regions in the Philippines; these regions being vastly different in several aspects [32]. Basically, we formulated and validated a mathematical model that is flexible enough to simulate the subtle and significant differences among select regions in the country.

Taking into account the influences of the different imposed quarantine levels, we focused on three distinct regions in the Philippines with different demographical, political, and environmental profiles: (1) National Capital Region (NCR), with an area of 619.54 square km [33], a highly urbanized and densely populated region; (2) Davao City, with area of 2443.61 square km [34], a culturally diverse city located in the southern region of the Philippines; and (3) Baguio City, with area of 57.51 square km [34], a densely populated city with high elevation and cold climate. Fig. 1 shows where these three regions-of-interest are located in the Philippines. Geographically, NCR and Baguio City are both located in Luzon island, the northern part of the Philippines with NCR located in the southwest portion

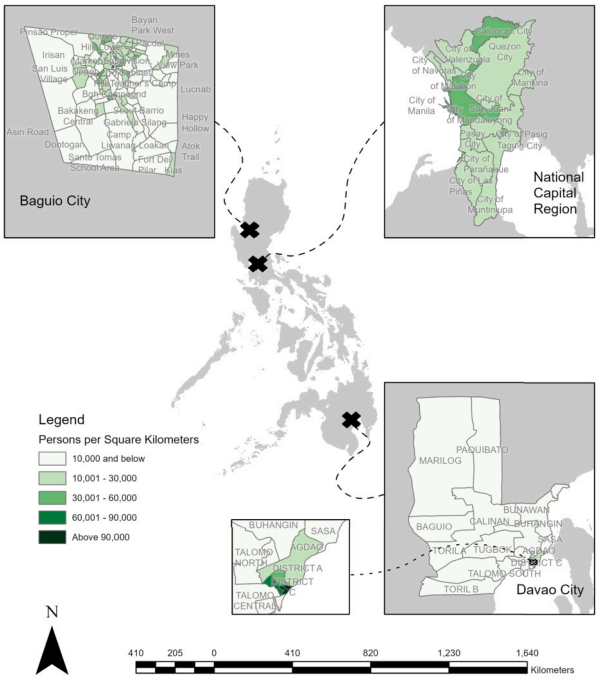

Fig. 1. Map of the locale of the study showing the three regions-of-interest and their locations in the Philippines. Insets are geopolitical boundaries with population densities where Baguio City is subdivided by *barangays*, NCR by cities, and Davao City by Health Districts.

of Luzon and Baguio City in the northern part of Luzon. On the other hand, Davao City is located in Mindanao island, the southern part of the Philippines. As shown in Fig. 1, the regions-of-interest are subdivided into different geopolitical domains. NCR is subdivided into different highly urbanized cities, Davao is subdivided into different health districts, while Baguio City is subdivided into the smallest political unit in the Philippines called *barangays*. Furthermore, the studied regions differ in population densities vastly affecting the transmission rates. As shown in Fig. 1, all of the cities in NCR are highly populous while the densest population in Davao City is only concentrated in a few of health districts, and the population of Baguio City is sparsely distributed across several *barangays*.

In controlling the spread of COVID-19, the regions-of-interest implemented community quarantines of different levels and durations. NCR implemented ECQ (March 16-May 15, 2020), MECQ_1 (May 16-May 31, 2020), GCQ_1 (June 1-August 3, 2020), MECQ_2 (August 4-18, 2020), and GCQ_2 (August 19, 2020) [35]. Davao City implemented ECQ (March 28-May 15, 2020), GCQ_1 (May 16-June 30, 2020), MGCQ (July 1-November 19, 2020), and GCQ_2 (November 20-ONWARDS, 2020) [36]. Meanwhile, Baguio City implemented MGCQ starting on July 15, 2020 towards the entirety of the pandemic with revisions to its protocols on September 1, October 1, October 23, and December 1, 2020 [37–41].

With the apparent differences in COVID-19 management and local-specific geopolitics and demographics, this paper aimed to develop a minimal model that captures the temporal transmission dynamics of COVID-19 across different regions in the Philippines and identify key epidemiological parameters affecting its prevalence despite implemented control interventions. We assessed the goodness-of-fit of the model in estimating the spread of the pathogen and the respective local differences on implementation, demographics, spatiotemporal, among other factors. In Section 2, we show the methodology of the study, specifically model development, the reproduction number, model fitting, and model projections. Sections 3 and 4 discuss the different results and expound on their implications as well as its conclusion, respectively.

2. Methodology

2.1. Model development

We considered modifying the classical Susceptible-Exposed-Infected-Recovered ($SEIR$) compartmental model implemented using coupled first-order differential equations. The system of the modified $SEIR$ model is shown in Equation (1) and its corresponding model diagram is presented in Fig. 2.

$$\frac{dS^i}{dt} = -g^i(t)\beta^i S^i \frac{\left(I_r^i + \sigma^i I_u^i\right)}{N^i},$$

$$\frac{dE^i}{dt} = g^i(t)\beta^i S^i \frac{\left(I_r^i + \sigma^i I_u^i\right)}{N^i} - \alpha^i E^i,$$

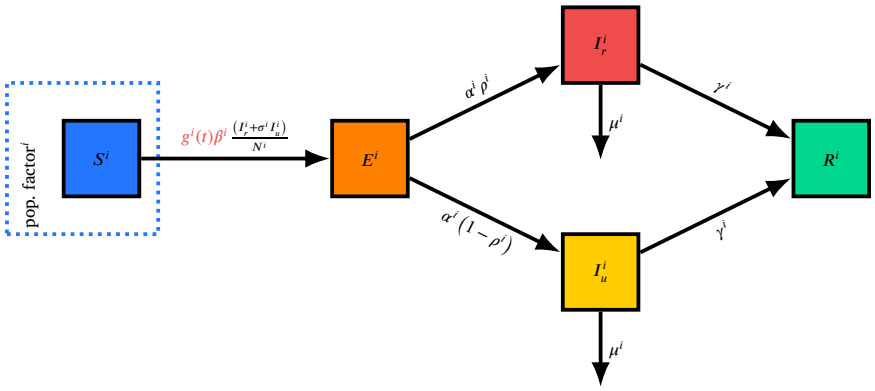

Fig. 2. The diagram of the modified SEIR model. The compartments of the model are shown as follows with the rates labeling the arrows. Population states are represented as solid boxes. Arrows represent the flow rates. Note that the S^i compartment is placed inside a broken rectangle to indicate that the Susceptible population varies according to population factor. The parameter $g^i(t)$ is a function of time t and is differentiated among other parameters. All of the factors in this model are piecewise functions to i: the quarantine level implemented.

$$\begin{aligned}
\frac{dI_r^i}{dt} &= \alpha^i \rho^i E^i - \mu^i I_r^i - \gamma^i I_r^i, \\
\frac{dI_u^i}{dt} &= \alpha^i \left(1-\rho^i\right) E^i - \mu^i I_r^i - \gamma^i I_r^i, \\
\frac{dR^i}{dt} &= \gamma^i \left(I_r^i + I_u^i\right),
\end{aligned} \tag{1}$$

for $i \in \{1, 2, ..., m\}, m \leq 5, m \in \mathbb{N}$ where i is the corresponding quarantine level and m is the total number of quarantine levels implemented per region.

The effect of the implemented intervention protocol is represented by the time-dependent parameter $g^i(t)$ which is modeled by a sigmoid function shown in Equation (2) [42]:

$$g^i(t) = \frac{g_0^i}{1 + \exp\left(\frac{-\left(t - t^i_{NPI}\right)}{t^i_\beta}\right)}. \tag{2}$$

The function $g^i(t)$ is initialized by the parameter t^i_{NPI} that serves as the starting day of the implementation of the community quarantine. The sigmoid ascends with the value of t^i_β that signifies the number of days from t^i_{NPI} that the intervention will take effect. This will cap off at a maximal value of g_0^i, deemed as the maximum percentage of *interacting population* for that community quarantine. Observe that when $t = t^i_{NPI}$, $g^i(t^i_{NPI}) = 0.5 * g_0^i$ and when $t \to \infty$, $g^i(t) \to g_0^i$. Fig. 4 illustrates the time-dependent parameter g across different regions and community quarantine periods, depicted by the black solid curve. The area under this curve represents the proportion of the population that remains interactive during the interventions. Within each quarantine period, the curve g displays a sigmoidal shape, eventually reaching a maximum value defined by g_0^i. This scenario is relevant to the Philippine context, as on the day a new community quarantine is implemented ($t = t^i_{NPI}$), there is an apparent stigma against movement among the interacting population and quarantine enforcers. This results in a lockdown that is effectively stricter than the one officially mandated. As time progresses ($t \to \infty$), this stigma gradually diminishes. Consequently, the actual interacting population will eventually reach the maximum allowed number (g_0^i) specified under the applied community quarantine.

Per quarantine i, the model initializes with a *population factor*: a certain percentage of the population that is at risk of contracting the disease due to frequent interactions with the public (e.g., frontliners, household representatives, etc.). The type of community quarantine implemented influences this population factor which limits the allowable population and is assumed to be constant throughout CQ implementation. The population factor directly affects the initial susceptible population (S_0^i) influencing the total population (N^i) for each i. Mathematically, the initialization for the S^i compartment per quarantine level i is represented as $S_0^i = g_0^i \cdot N^i$.

In System (1), the transmission is brought about by the interaction of the reported (I_r^i) and unreported (I_u^i) infectious compartments to susceptibles (S^i) at a transmission rate β^i. This causes the infected susceptible to move into the exposed (E^i) compartment. A factor σ^i to the unreported cases indicates the multiplicative transmissibility of these unreported cases as these patients are unaccounted for and are basically at large.

The exposed compartment has a latency rate α^i whose reciprocal is the incubation period of the virus until the patients become infectious. The infectious population is subdivided into two compartments, namely I_u^i (unreported) and I_r^i (reported) with ρ^i as the proportion of reported infectious cases. This parameter also reflects the protocol of stringent testing and tracing to identify the cases.

Table 1
Assigned values of the population factor, interacting population, and day of implementation for each community quarantine period.

Region	i	Community Quarantine	Population Factor	Interacting population, g_0^i	t_{NPI}, in the year 2020
NCR	1	ECQ	10%	25%	March 16
	2	$MECQ_1$	20%	50%	May 16
	3	GCQ_1	40%	75%	June 1
	4	$MECQ_2$	30%	50%	August 4
	5	GCQ_2	60%	75%	August 19
Davao City	1	ECQ	25%	15%	March 28
	2	GCQ_1	50%	40%	May 16
	3	MGCQ	85%	65%	July 1
	4	GCQ_2	60%	50%	November 20
Baguio City	1	$MGCQ_1$	50%	55%	July 15
	2	$MGCQ_2$	60%	65%	September 1
	3	$MGCQ_3$	70%	75%	October 1
	4	$MGCQ_4$	60%	65%	October 23
	5	$MGCQ_5$	80%	85%	December 1

Then, the infectious compartments either recover (R^i) or die (D^i) at the rates γ^i and μ^i, respectively. The differential equation for the deceased compartment is $\frac{dD^i}{dt} = \mu^i \left(I_r^i + I_u^i\right)$. Hence, the differential equation of the total population is $\frac{dN^i}{dt} = -\mu^i \left(I_r^i + I_u^i\right)$.

2.2. Time-varying reproduction number R_t

The closed form of the compartmental time-varying reproduction number R_t was derived using the next generation matrix method [43]. To see if the model reasonably captures the cases, we compared the results from the time-varying reproduction number R_t to the statistical R_t generated using the R package EpiEstim [44].

2.3. Data and model fitting

The developed model was fitted to the 7-day moving average of confirmed daily cases per selected region: the NCR, Davao City, and Baguio City. The data used for NCR were obtained from the Department of Health Data Drop [45]. For Davao City, data was obtained, under non-disclosure and data sharing agreements, from the Regional Epidemiology Surveillance Unit of the Department of Health - Davao Center for Health Development. Similarly, the data for Baguio City was obtained from the Epidemiological Surveillance Unit of the Baguio City Health Services Office.

In this study, the model parameters β^i, ρ^i, and μ^i were estimated using the nonlinear least-squares fitting technique [46]. Using this method, the model solution was fitted to the moving average of daily COVID-19 incidences by finding the set of parameter values that minimizes the sum of squared differences between COVID-19 cases and the model solution. This sum of squared differences is generally formulated as an objective function,

$$Z^i = \arg\min_{P^i \in B} \sum_{j=1}^{n} \left(f(t_j; P^i) - y(t_j)\right)^2, \tag{3}$$

where $P^i = (\beta^i, \rho^i, \mu^i)$ in the three-dimensional space B defined by the respective parameter bounds, t_j are the time points of COVID-19 cases data, $f(t_j; P^i)$ is the model solution, and $y(t_j)$ are the moving average data for COVID-19 cases. Thus, we want to find the best fit to the data indicated as $f(t_j; P^i)$.

The model fitting procedure was done in Matlab using the `lsqcurvefit` function [47]. The method used for numerical optimization in solving non-linear least squares problem was the trust-region reflective algorithm. For the three regions under study, a piecewise model-fitting approach was performed, wherein the time-series data was divided into m different periods that corresponded to the community quarantine level implemented, as shown in Table 1. Consequently, there will be different sets of estimated parameters per ith period, $i \in \{1, 2, ..., m\}$.

To estimate the other model parameters, the different scenarios and circumstances per region were taken into account to simulate the dynamics of the COVID-19 transmission. Following the geopolitical, demographical and temporal factors of each region, the initial model parameter values are shown in Tables 1 and 2.

2.4. Short-term projections

The data was subdivided into fitting data and test data for verification. For the projections, the fitting data is obtained from the last quarantine periods of Aug 19, 2020 - Dec 31, 2020, Nov. 20, 2020 - Jan. 31, 2021, and Dec 1, 2020 - Dec 31, 2020, for NCR, Davao City, and Baguio City, respectively. After the model parameters have been calibrated according to the respective regions-of-interest and periods, the model is validated by comparing the predictions with the test data. The testing periods were Jan 1-15, 2021, Feb 1-15, 2021, and Jan 1-15, 2021 for NCR, Davao City, and Baguio City, respectively. This step involves projecting the COVID-19

Table 2
Assumed parameter values per region-of-interest.

Region	α^i (day^{-1})	t^i_β (days)	σ^i	γ^i (day^{-1})	E^i_0 (indv)	$I^i_{R_0}$ (indv)
NCR	0.2	14	1.5	$\frac{1}{14}$	2500	250
Davao City	0.2	3	2	$\frac{1}{13}$	700	250
Baguio City	0.2	14	2	$\frac{1}{16}$	100	25

cases for the next 15 days using the calibrated model and comparing it with the actual data. The projections were done for different values of g^i_0 $(25\%, 50\%, 75\%, 100\%)$, simulating scenarios of community quarantine. The result was then subjected to bootstrapping techniques with 10,000 samples to construct confidence intervals around the model predictions.

3. Results and discussion

3.1. Reproduction number

Using the next generation matrix method, the deterministic time-varying reproduction number (R_t) is derived as follows:

$$R^i_t = \frac{\beta^i g^i(t)(\rho^i + \sigma^i(1-\rho^i))S^i(t)}{(\mu^i + \gamma^i)N^i(t)}. \tag{4}$$

The detailed calculation is provided in the supplemental file. R^i_t is a dimensionless parameter that represents the balance between the transmission of the infection and the removal of infected individuals from the population. Hence, $g^i(t)$ is directly proportional to R^i_t which implies that the implemented initial mobility restrictions have a direct effect on the spread of the contagion. Similarly, the β^i parameter is directly proportional to R^i_t, which implies that protocols designed to lessen transmission, such as wearing of face masks and proper hygiene, will have a direct effect on transmission mitigation.

As seen in Fig. 3, the derived deterministic R^i_t follows the trend of the statistical R^i_t. It is noteworthy to say that the deterministic R^i_t over statistical R^i_t trends in Davao City appears more similar compared to NCR and Baguio City. This discrepancy could be attributed to the data source as Davao City's data is validated by its Regional Epidemiology Unit which verified the actual onset of symptoms, among other indicators used in the study. The Baguio City data was obtained from the Epidemiological Surveillance Unit of the Baguio City Health Services Offices but aside from the timely release of data, its validation and verification was insufficient. Meanwhile, the data for NCR was obtained from the National Data drop. However, some data points were difficult to validate, and certain cases were reported in bulk. Nevertheless, the model was still able to capture the overall trend despite the data limitations.

3.2. Model fitting and epidemiological parameter values

The results from the sensitivity analysis identified the parameters β^i, ρ^i, μ^i and g^i_0 as key parameters driving the transmission dynamics (see Supplemental file Section C). As g^i_0 depends on the issued community quarantine per area of interest, it was not estimated but instead aligned with the respective proportions of the interacting population and the ratio of compliant to non-compliant individuals according to each quarantine protocol during the specified period (see Table 1 and Fig. 4). In NCR, the highest interacting population of 75% was observed during GCQ_2, while the lowest interacting population of 25% was observed during ECQ. The population factor was lowest during ECQ at 10% and highest during GCQ_1 at 40%. In Davao City, the highest interacting population was observed during MGCQ at 85%, while the lowest interacting population of 15% was observed during ECQ. The population factor was lowest during ECQ at 25% and highest during MGCQ at 85%. In Baguio City, the highest interacting population was observed during $MGCQ_5$ at 80%, while the lowest interacting population of 55% was observed during $MGCQ_1$. The population factor was lowest during $MGCQ_1$ at 50% and highest during $MGCQ_3$ at 70%. The findings of this study suggest that community quarantine measures can significantly impact the interacting population and the population factor, which can subsequently affect the transmission of COVID-19. These results are consistent with previous studies that have reported reduced mobility during stricter quarantine measures, leading to decreased transmission rates [48,49]. However, it is important to note that these measures may have economic and social consequences that need to be considered when implementing them. Hence, careful consideration is needed in determining the appropriate level of community quarantine measures to balance the prevention of COVID-19 transmission and the economic and social needs of the community.

The transmission multiplicative factor σ^i of untraced cases was estimated to be 1.5 in NCR and 2 in Davao and Baguio City (see Table 2). Fig. 5 supports this assumption as it shows that the respective chosen value makes the model estimation convergent. This result indicates that an infected individual can infect two or more individuals in Baguio and Davao, while an infected individual can transmit the virus to 1.5 individuals in NCR.

Recall the assumed values of the epidemiological parameters in Table 2 for the three regions-of-interest. The latency rate, denoted by α^i, was 0.2 in all three regions. This indicates that, on average, it takes about five days for an infected individual to start showing symptoms of COVID-19 and become infectious. The recovery rate, denoted by γ^i, was 0.0625, 0.0769, and 0.0714 in Baguio, Davao, and NCR, respectively. This suggests that it takes about 16 days for an infected individual to recover from COVID-19 in Baguio, while it takes approximately 13 days in Davao and 14 days in NCR.

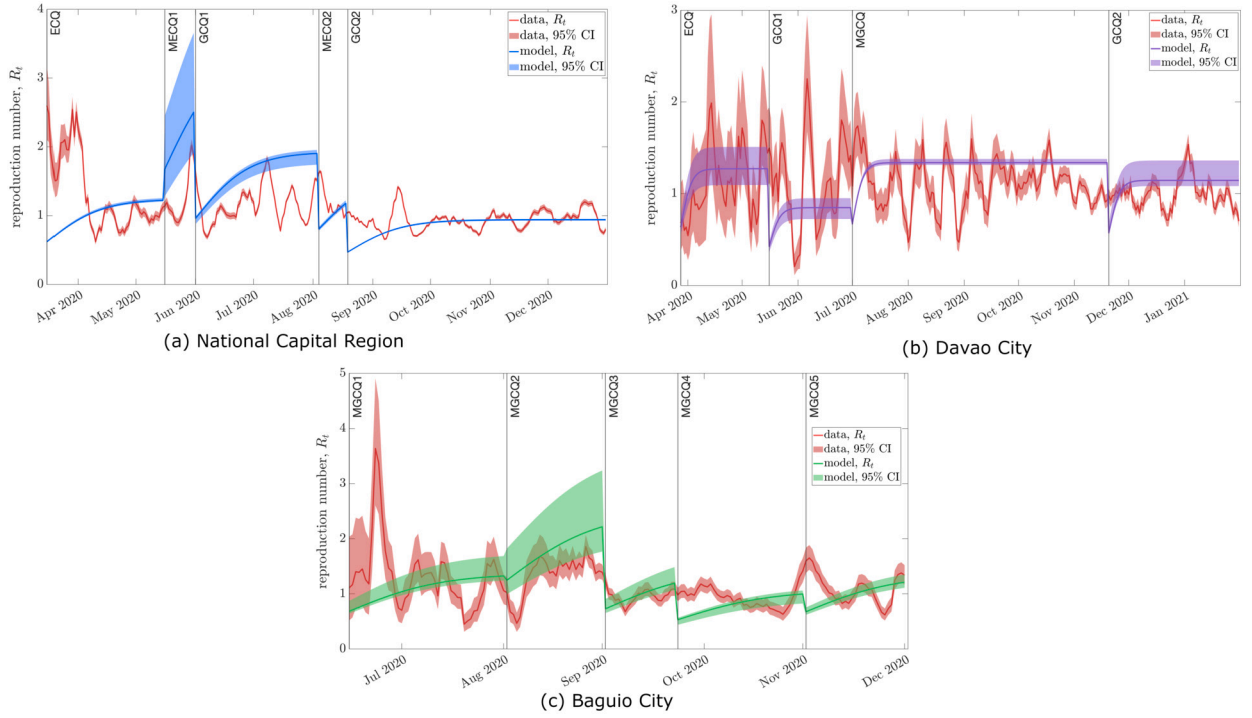

Fig. 3. Comparison of the deterministic time-varying reproduction number over the statistical R_t in (a) National Capital Region, (b) Davao City, and (c) Baguio City. The statistical reproduction number (red) is computed using the data for the day-to-day cases of the three regions-of-interest. In contrast, the reproduction number of the model from simulations (shown in blue for (a), purple for (b), and green for (c) are plotted with their respective 95% confidence interval. For all regions, differences between the model R_t and the statistical R_t can be observed in some periods. In (a), the model and statistical R_t showed different trends at the beginning of ECQ but became similar at the end of the period; in (b), statistical R_t during GCQ_1 reaches less than 1 then goes up to approximately 3 in some days, while model R_t increased but remained to be less than 1; in (c), the model and statistical R_t showed different trends during $MGCQ_4$. Moreover, model and statistical R_t exceed 1 throughout different periods in all regions, which means that there is indeed a disease spread.

The estimated i_β^i for the NCR, Davao City, and Baguio City were 14, 3, and 14, respectively. This means that the mobility interventions implemented in these regions could take approximately two weeks to take effect in the NCR and Baguio City, while it could take up to three days in Davao City. These findings are consistent with previous studies that have reported the effectiveness of mobility interventions, such as lockdowns and travel restrictions, in reducing the spread of COVID-19 [50].

Using the assumed values, the model fitting procedure was conducted to derive the values for β^i, μ^i, and ρ^i parameters as reflected in Table 3. Fig. 9 in the Supplemental file shows the corresponding histogram of the estimated parameters. The results indicate that in NCR, the highest transmission rate was observed during the ECQ implementation ($\beta^1 = 0.893$ day^{-1}), followed by MECQ$_1$ ($\beta^2 = 0.62$ day^{-1}), MECQ$_2$ ($\beta^4 = 0.452$ day^{-1}), GCQ$_2$ ($\beta^5 = 0.169$ day^{-1}), and GCQ$_1$ ($\beta^3 = 0.129$ day^{-1}). The death rate was highest during ECQ ($\mu^1 = 0.221$ day^{-1}) and MECQ$_2$ ($\mu^4 = 0.171$ day^{-1}), and lowest during GCQ$_1$ ($\mu^3 = 0.016$ day^{-1}). The estimated underreporting ($1-\rho^i$) was highest during GCQ$_1$ (72.61%) and lowest during ECQ (62.41%). In Davao City, the highest transmission rate was observed during ECQ ($\beta^1 = 0.473$ day^{-1}), followed by GCQ$_1$ ($\beta^2 = 0.174$ day^{-1}), MGCQ ($\beta^3 = 0.136$ day^{-1}), and GCQ$_2$ ($\beta^4 = 0.136$ day^{-1}). The death rate was highest during GCQ$_1$ ($\mu^2 = 0.082$ day^{-1}) and lowest during ECQ ($\mu^1 = 0.032$ day^{-1}). The estimated underreporting was highest during ECQ (97.02%) and lowest during MGCQ (91.78%). In Baguio City, the transmission rate was highest during MGCQ$_1$ ($\beta^1 = 0.55$ day^{-1}) and lowest during MGCQ$_3$ ($\beta^3 = 0.373$ day^{-1}). The death rate was highest during MGCQ$_4$ ($\mu^4 = 0.333$ day^{-1}) and lowest during MGCQ$_2$ ($\mu^2 = 0.085$ day^{-1}). The estimated underreporting was highest during MGCQ$_3$ (64.89%) and lowest during MGCQ$_5$ (29.25%).

The results of this study suggest that the transmission rate, death rate, and estimated underreporting vary across different locations and community quarantine implementations in the Philippines. The highest transmission rates per region-of-interest were observed during $i = 1$ (ECQ in NCR and Davao City, and MGCQ$_1$ in Baguio City). These estimates are consistent with the fact that these community quarantines are the first to be implemented in each region when much information on the biology and transmission dynamics of the virus is yet to be gleaned, hence most of the effective intervention strategies are yet to be identified.

The highest death rate was observed during ECQ ($i = 1$) in NCR, GCQ$_1$ ($i = 2$) in Davao City, and MGCQ$_4$ ($i = 4$) in Baguio City. These periods coincide with the availability of caring facilities per region and the population. The NCR, despite having more hospitals, has the most densely populated cities that the hospital beds and healthcare facilities were overwhelmed immediately at the onset of the pandemic coupled with the immediate lack of medicines and other life-support amenities due to the influx of cases. Meanwhile, Davao City, having been situated in the southern part of the country, got a delayed influx of cases compared to NCR and hence had some time to prepare its resources and its intervention strategies resulting to a fairly lower death rate on the first period of CQ implementation. Nevertheless, as it still has millions of residents, its cases still rose and had its hospitals and healthcare

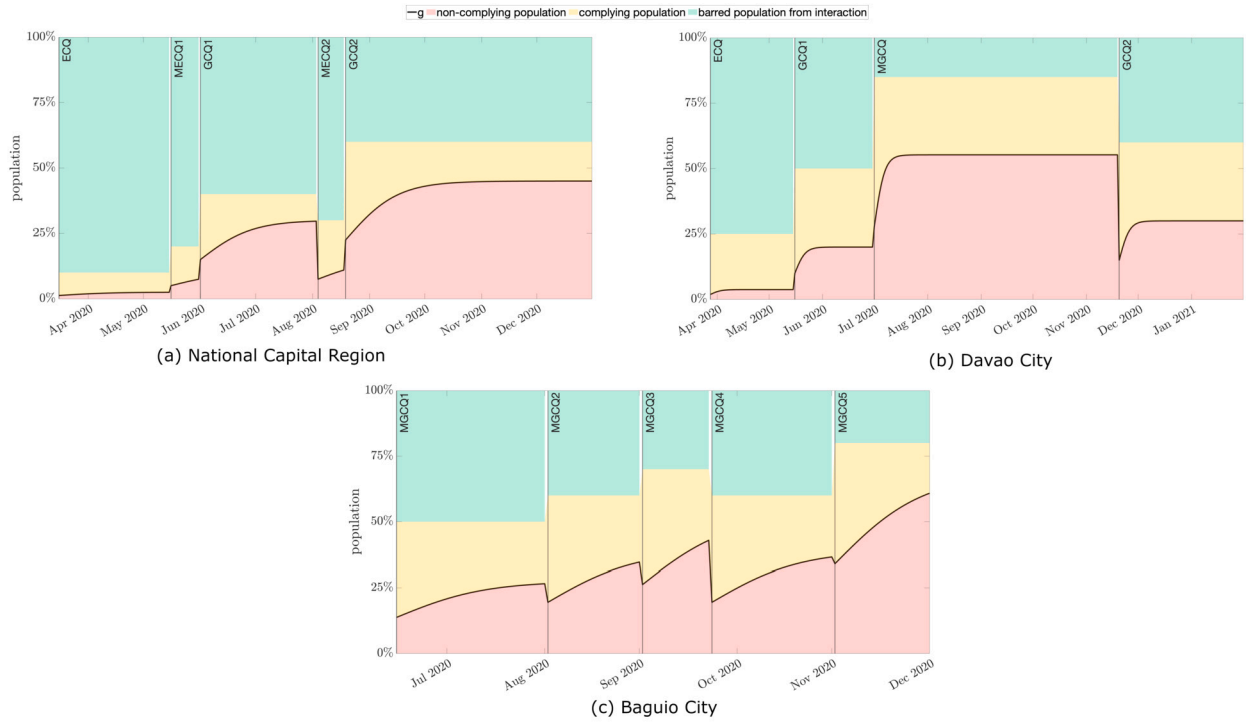

Fig. 4. Visualizing the concept of population factor and the g parameter for NPIs for (a) National Capital Region, (b) Davao City, and (c) Baguio City. For (a), (b), and (c), shown in green is the portion of the population not considered in the model for each community quarantine. The remaining population is further divided using the g parameter (black curve) that labels the time-varying populations that are compliant (in yellow) and not compliant (in red) to the quarantine.

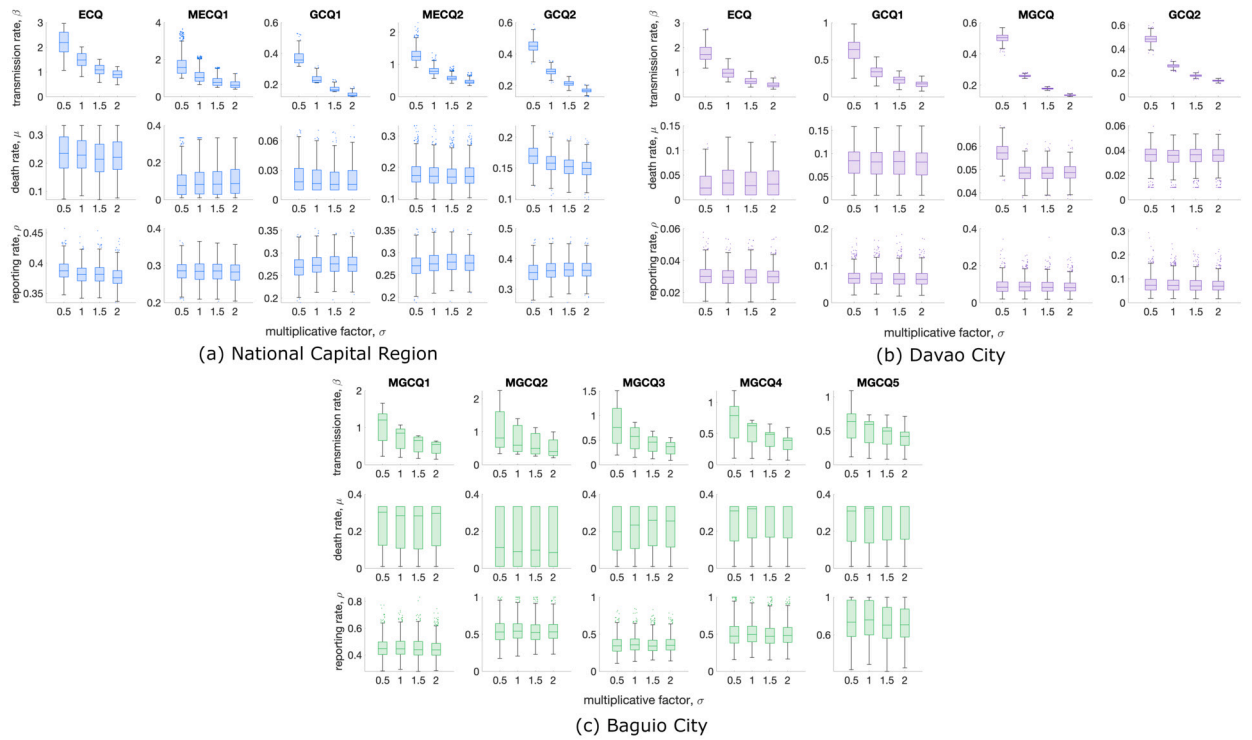

Fig. 5. Comparing the estimated parameters for selected values of multiplicative factors σ in (a) National Capital Region, (b) Davao City, and (c) Baguio City. For σ values of 0.5, 1.0, 1.5, and 2.0, each community quarantine (in columns) is shown with the box plots of their respective parameters: (top row) transmission rate, β, (middle row) death rate, μ, and (bottom row) reporting rate, ρ.

Table 3
Estimated parameter values and 95% confidence intervals per region-of-interest and intervention.

Region	i	Community Quarantine	β^i(day^{-1})	μ^i(day^{-1})	ρ^i(%)
NCR	1	ECQ	0.893 (0.584 – 1.215)	0.221 (0.112 – 0.333)	37.59 (35.01 – 41.07)
	2	$MECQ_1$	0.62 (0.429 – 1.205)	0.086 (0.01 – 0.333)	28.28 (22.61 – 33.14)
	3	GCQ_1	0.129 (0.122 – 0.164)	0.016 (0.01 – 0.05)	27.39 (23.27 – 32.24)
	4	$MECQ_2$	0.452 (0.366 – 0.633)	0.171 (0.12 – 0.269)	27.7 (23.12 – 32.75)
	5	GCQ_2	0.169 (0.145 – 0.194)	0.149 (0.119 – 0.179)	36.25 (30.65 – 42.52)
Davao City	1	ECQ	0.473 (0.355 – 0.699)	0.032 (0.01 – 0.096)	2.98 (1.95 – 4.22)
	2	GCQ_1	0.174 (0.088 – 0.236)	0.082 (0.01 – 0.132)	6.32 (3.4 – 11.64)
	3	MGCQ	0.136 (0.129 – 0.143)	0.049 (0.042 – 0.056)	8.22 (3.57 – 16.78)
	4	GCQ_2	0.136 (0.119 – 0.146)	0.036 (0.017 – 0.047)	6.96 (2.94 – 14.49)
Baguio City	1	$MGCQ_1$	0.55 (0.161 – 0.627)	0.296 (0.01 – 0.333)	43.81 (33.4 – 61.63)
	2	$MGCQ_2$	0.402 (0.241 – 0.87)	0.085 (0.01 – 0.333)	53.16 (30.61 – 81.65)
	3	$MGCQ_3$	0.373 (0.118 – 0.498)	0.2556 (0.01 – 0.333)	35.11 (19.6 – 61.22)
	4	$MGCQ_4$	0.391 (0.108 – 0.505)	0.333 (0.038 – 0.333)	48.43 (26.43 – 84.24)
	5	$MGCQ_5$	0.416 (0.125 – 0.647)	0.333 (0.025 – 0.333)	70.75 (37.33 – 100.0)

facilities overwhelmed on the second CQ implementation. Baguio City, on the other hand, despite having the highest death rate only on $MGCQ_4$, it consistently had the highest death rates compared to NCR and Davao City. This difference can be attributed to Baguio's aging population, its lower temperature (lowest in the country), higher elevation, dense population and having the fewest number of hospitals among the regions-of-interest.

The reporting ratio, ρ^i, represents the proportion of actual COVID-19 cases that are reported by the health care system. It is equal to one minus the estimated underreporting in the population. A high reporting ratio indicates that the health care system is capturing a larger proportion of COVID-19 cases in the population, while a low reporting ratio suggests that many cases are going undetected. In the context of the COVID-19 pandemic, underreporting is a significant challenge that makes it difficult to accurately estimate the true burden of the disease in a population. Factors such as limited testing capacity, asymptomatic cases, and mild or moderate symptoms can contribute to underreporting. Now, as seen in Table 3, the estimated underreporting was highest during ECQ in all locations, while the lowest estimated underreporting was observed during $MGCQ_5$ in Baguio City. It is noteworthy that Davao City had the highest range of underreporting (91.78-97.02%) among these regions. This observation is due to the fact that Davao City has the largest area in the Philippines. This wide area and sparsely distributed populace pose significant problem in tracking cases and their possible contacts given the very few testing facilities during that quarantine period. A higher reporting ratio, such as the one observed in Baguio City in $MGCQ_5$, suggests that the health care system is detecting a larger proportion of COVID-19 cases in the population. This can be attributed to a variety of factors, such as an effective testing strategy, high public awareness and adherence to public health measures, and effective contact tracing. Conversely, a lower reporting ratio, such as the one observed in NCR in GCQ_1, implies that the actual number of COVID-19 cases in the population is likely higher than the reported number. Note that NCR is known for its dense population and diverse geopolitical structure which can be barriers in implementing COVID-19 control interventions and detection. Hence, we infer that the low reporting ratio of NCR can be attributed to low adherence to public health measures.

Fig. 6 shows that the resulting model curves follow the general trend of cases in each area of interest per community quarantine implemented. This further supports the flexibility and robustness of the model to capture the dynamics of the spread despite the differences in circumstances of every region-of-interest.

3.3. Projections

To verify the validity of the compartmental model in predicting the spread of COVID-19, we conducted short-term projections for the next 15 days using the calibrated model. The forecast was simulated according to different interacting population scenarios that reflect the supposed quarantine protocol implemented. The results are shown in Fig. 7.

Simulation results shown in Fig. 7 revealed that the model was able to capture the trend in the actual test data for the next 15 days with reasonable accuracy. The predicted number of infected cases closely followed the actual data, and the confidence intervals around the predictions were relatively narrow, indicating that the model was able to produce reliable predictions. We also observed that the effectiveness of the quarantine protocol significantly influenced the spread of the virus. The model predicted that a strict quarantine protocol with a g_0^i of 25% would result in a significant decrease in the number of infected cases, while a less strict protocol with a g_0^i of 100% would result in a rapid increase in the number of infected cases.

Projection results indicate that the model was able to accurately anticipate the COVID-19 cases within a relatively narrower intervals compared to projections based on data-hungry and time series-dependent methods like that of Parikshit et al., 2022 [51] where they projected the cases to be between 601,220-664,506 but the actual reported cases was just 360,775. The discrepancies can be further attributed to the use of moving averages in the entirety of the dataset without accounting for differences of protocols and doing piece-wise fitting procedures. In the context of the Philippines, the differences in the implemented CQ and the geopolitical, demographical and socio-economic nuances would render significant challenges in the projections. Nevertheless, despite the differences in the modeling framework, our projections corroborate with the results of de Lara-Tuprio et al., 2022 [52] where instead of projections based on g_0, they adjusted the force of infections to simulate changes in the number of interacting populations and

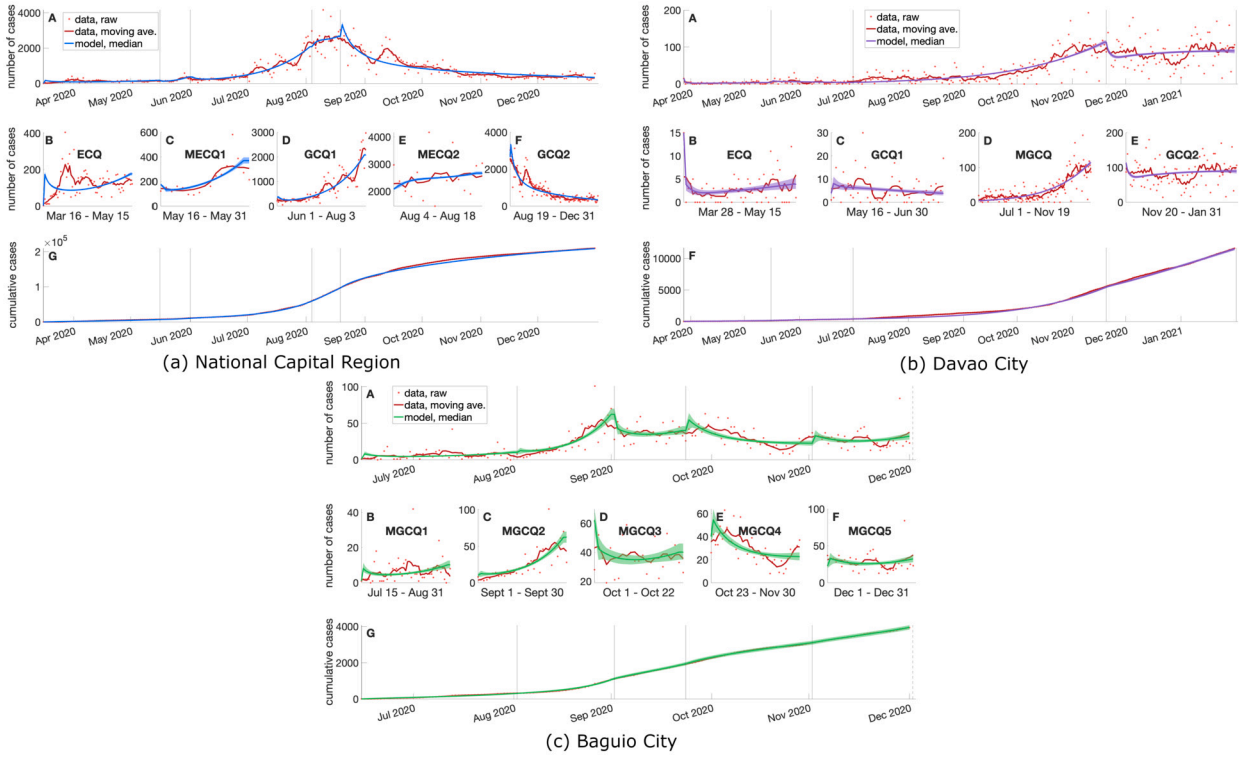

Fig. 6. The data and the model for the COVID-19 incidences in the (a) National Capital Region, (b) Davao City, and (c) Baguio City. The reported cases per day (red dotted), its 7-day moving average (red line), and the model fit (shown in blue, purple, and green, respectively) are shown in (A) with their corresponding CQ divisions in (B-F) for NCR and Baguio and (B-E) for Davao City. The cumulative cases are plotted with their corresponding model fit in (G) for NCR and Baguio and (F) for Davao City.

scenarios of a series of CQs to be implemented. Both forecasts support policy recommendations for preferred scenarios and informed preparations.

It is noteworthy to mention that our findings align with and build upon recent studies on COVID-19 transmission dynamics. For instance, recent mathematical models have incorporated time-dependent parameters to capture various phases influenced by public health interventions, changing contact patterns, and demographic shifts [20–22]. By incorporating the function $g^i(t)$ in our model, we capture similar dynamics, showing how varying quarantine levels influence interaction rates and disease transmission over time. This approach echoes studies that model higher-order interactions, such as non-pharmaceutical interventions through networks [25,26].

Furthermore, our modeling approach is validated by comparing the derived time-varying reproduction number (R_t) with the statistical R_t values calculated using real-world data. This comparison provides confidence that our model accurately reflects observed trends, demonstrating robustness similar to the approaches used in recent literature. Thus, our study contributes to the existing body of work on epidemic modeling, offering a context-specific analysis tailored to the regions in the Philippines.

4. Conclusion

Effective management strategies are critical to mitigate the impact of the COVID-19 pandemic. Targeted, context-specific interventions are key to systematically and economically reduce the adverse effects of disease spread. In this study, we modeled and analyzed the COVID-19 transmission dynamics to derive relevant epidemiological parameters and their values for three regions of the Philippines, namely the National Capital Region (NCR), Davao City, and Baguio City, under different community quarantine implementations. The sensitivity analysis of the formulated model distinguishes the parameters β^i, ρ^i, μ^i, and g_0^i as parameters that need to be reliably estimated. The interacting population g_0^i had been tailored to the respective implemented community quarantine per area of interest. The interacting population differs across regions-of-interest as population density and resources varies.

Our analysis shows that the transmission rate, β^i, is affected by the level of community quarantine implementation. Since β^i is expressed as day^{-1}, indicating the number of people an infected individual can transmit the virus to per day, the higher its value, the faster the virus can spread through the population. Hence, policymakers should use β^i as a key indicator in monitoring the spread of COVID-19 and making informed decisions on quarantine measures. It is important to note that transmission rates are observed to be highest during the first onset of the pandemic. Therefore, quick implementations of intervention protocols during the first outbreak are highly recommended to ease the disease burden.

The death rate, μ^i, is another important metric to evaluate the severity of COVID-19 and the effectiveness of interventions in reducing mortality. Our analysis shows that the death rate varied across different regions, with the highest death rate observed in NCR

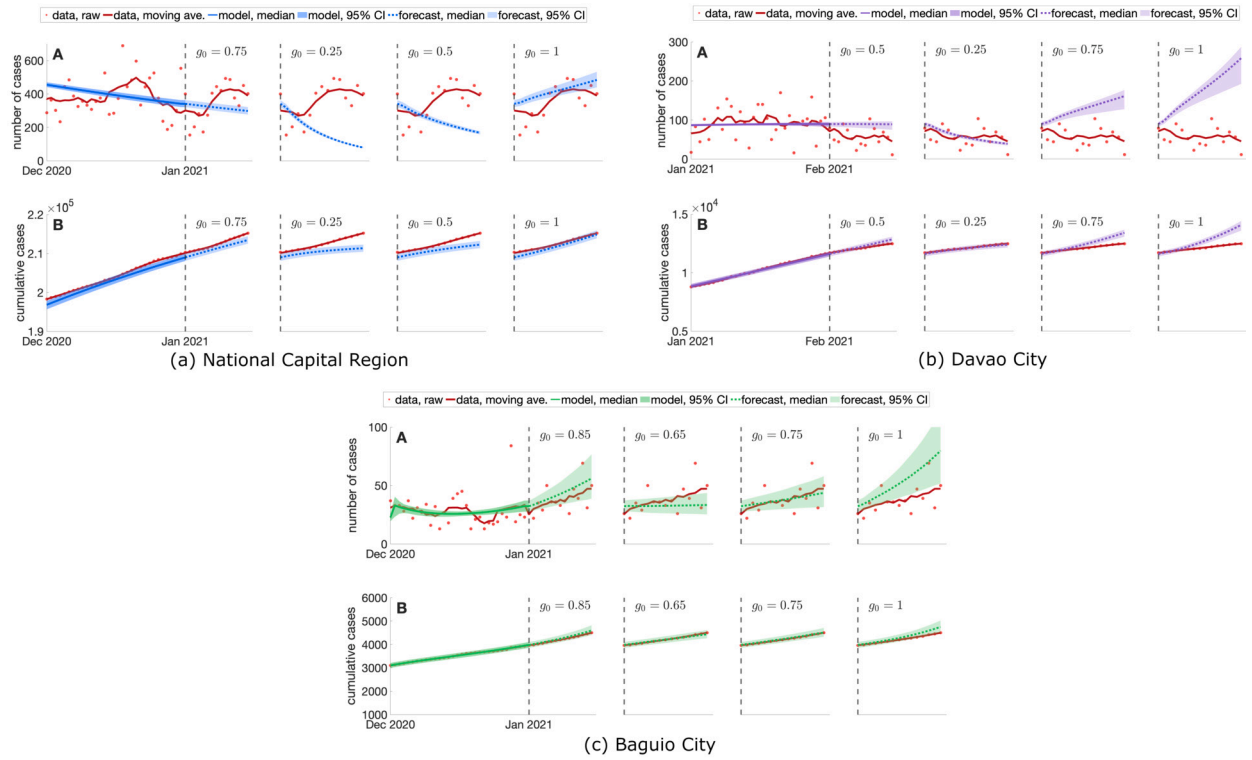

Fig. 7. 15-day forecasting for (a) National Capital Region, (b) Davao City, and (c) Baguio City. Shown are the data (red) and the model (blue for (a), purple for (b), and green for (c)) for (A) the day-to-day number of cases and (B) the cumulative cases for the 15-day forecasting from January 1, 2021 to January 15, 2021 for (a) and (c) and from February 1, 2021 to February 15, 2021 for (b). Scenarios of unchanged $g_0 = 0.75, 0.5$, and 0.85 for (a), (b), and (c), respectively, and varying values of $g_0 = 0.25, 0.5$, and 1.0 for (a), $g_0 = 0.25, 0.75$, and 1.0 for (b), and $g_0 = 0.65, 0.75$, and 1.0 for (c), are also illustrated.

during ECQ, indicating a higher risk of mortality among infected individuals. In contrast, Davao City had a relatively low death rate throughout the different community quarantine phases, suggesting that the healthcare system was effective in managing the disease. Moreover, comparing the death rates between different regions can provide insights into the efficacy of their respective healthcare systems in managing COVID-19. A lower death rate in a region may suggest better access to healthcare facilities, adequate medical supplies, and effective treatment protocols. On the other hand, a higher death rate may indicate a healthcare system overwhelmed with cases, inadequate medical resources, or less effective treatment protocols. Thus, providing sufficient amenities will help mitigate death tolls in future health crises. Overall, the death rate provides crucial information for policymakers and healthcare professionals in managing the COVID-19 pandemic, including decisions on the allocation of resources and implementation of interventions.

Furthermore, the reporting ratio, ρ^i, provides insights into the effectiveness of the health system in detecting and responding to COVID-19. Our analysis shows that the reporting ratio varied across different regions and community quarantine phases, with a higher reporting ratio observed in Baguio City during MGCQ_5, indicating an effective testing strategy and public awareness and adherence to public health measures. A high reporting ratio suggests that the health system is capturing a larger proportion of COVID-19 cases, which can aid in implementing appropriate interventions and mitigating the spread of the disease. Importantly, the reporting ratio is highly related to the geopolitical landscape of the region. That is why the LGU would play a crucial role in ensuring that this parameter is addressed and well-accounted for.

The short-term projections conducted in this study demonstrate the potential of compartmental models in predicting the spread of COVID-19 and assessing the effectiveness of control measures aiding public health policies and governance. However, modelers should exercise caution when using this model to predict COVID-19 cases in other regions, as it requires careful calibration with limited data. Our model has several key limitations. First, it is based solely on confirmed case and death data, lacking detailed information on exposed individuals and population interactions. It also assumes that transmission rates and the effectiveness of control measures remain constant over time, which may not reflect real-world conditions. Furthermore, the model does not incorporate age structure or spatial dynamics, both of which could affect the accuracy of the results. Future extensions could address these limitations by including the impact of other interventions, such as vaccination, a critical strategy in controlling the spread of the virus.

In summary, our research underscores the complex dynamics of quarantine measures on the control of COVID-19, highlighting their varying effects in different places. Due to its flexibility, simplicity and predictive power, this modeling framework has actually been utilized and was integrated into a decision-support system developed by local system developers. This web-based system serves as a virtual planning platform for policy makers to aid them in making informed decisions when managing and mitigating the spread of COVID-19. Policymakers are urged to tailor their strategies to the specific local context, recognizing the need for a nuanced and adaptable approach. A comprehensive decision-making process must weigh the advantages of such measures against

their economic and social ramifications, with a particular emphasis on mitigating adverse effects on vulnerable populations. This integrated perspective ensures a balanced and effective response to the ongoing challenges posed by the pandemic.

In conclusion, our study highlights the importance of community quarantine implementation, healthcare system effectiveness, and reporting ratio in managing the COVID-19 pandemic. The findings support the flexibility and robustness of the employed model to simulate the pathogen spread despite the topographical, climatic, socio-cultural, and demographical differences. Results of this study can aid policymakers and healthcare professionals in making informed decisions regarding interventions and resource allocation to mitigate the spread of the disease and reduce the associated morbidity and mortality. Future studies can build on our analysis by incorporating additional factors such as vaccination rates and genomic surveillance to provide a more comprehensive picture of the COVID-19 pandemic.

CRediT authorship contribution statement

May Anne E. Mata: Writing – review & editing, Writing – original draft, Visualization, Validation, Supervision, Resources, Project administration, Methodology, Investigation, Funding acquisition, Formal analysis, Conceptualization. **Rey Audie S. Escosio:** Writing – review & editing, Writing – original draft, Visualization, Software, Methodology, Investigation, Formal analysis, Data curation, Conceptualization. **El Veena Grace A. Rosero:** Writing – original draft, Visualization, Validation, Software, Methodology, Investigation, Formal analysis, Data curation, Conceptualization. **Jhunas Paul T. Viernes:** Writing – original draft, Visualization, Validation, Software, Methodology, Investigation, Formal analysis, Data curation, Conceptualization. **Loreniel E. Anonuevo:** Writing – review & editing, Validation, Software, Methodology, Investigation. **Bryan S. Hernandez:** Writing – review & editing, Validation, Supervision, Methodology, Investigation, Conceptualization. **Joel M. Addawe:** Validation, Supervision, Conceptualization. **Rizavel C. Addawe:** Writing – original draft, Validation, Supervision, Conceptualization. **Carlene P.C. Pilar-Arceo:** Writing – review & editing, Validation, Supervision, Project administration. **Victoria May P. Mendoza:** Writing – review & editing, Validation, Supervision, Methodology, Investigation, Conceptualization. **Aurelio A. de los Reyes:** Writing – review & editing, Writing – original draft, Visualization, Validation, Supervision, Software, Methodology, Investigation, Formal analysis, Data curation, Conceptualization.

Ethics approval

This study utilized secondary publicly available data without sensitive information. Hence, ethics review and approval was not necessary.

Declaration of generative AI and AI-assisted technologies in the writing process

During the preparation of the Conclusion section of this work the authors used ChatGPT in order to improve its readability. After using this tool/service, the authors reviewed and edited the content as needed and take full responsibility for the content of the publication.

Declaration of competing interest

The authors declare the following financial interests/personal relationships which may be considered as potential competing interests:

May Anne Mata reports financial support was provided by Republic of the Philippines Department of Science and Technology. May Anne Mata reports financial support was provided by University of the Philippines Resilience Institute. If there are other authors, they declare that they have no known competing financial interests or personal relationships that could have appeared to influence the work reported in this paper.

Acknowledgements

This project is funded by the University of the Philippines Resilience Institute (UPRI) under the Modeling and Simulation COVID-19 Project and is partially funded by the Department of Science and Technology - Philippine Council for Health Research and Development (DOST-PCHRD), under the Niche Center in the Region (NICER) Project: Predictive Modeling and Viral Phylodynamic Analysis on the Spatial and Temporal Patterns of Disease Outbreaks with Considerations for Control and Logistics applied in the Mindanao Region – (PPASTOL). The help of Mr. Federico T. Calo in creating the map of the research locale (Fig. 1) is also acknowledged.

Appendix A. Supplementary material

Supplementary material related to this article can be found online at https://doi.org/10.1016/j.heliyon.2024.e39330.

Data availability

Data used are publicly available at the Department of Health data drop [45].

References

[1] T. Struyf, J. Deeks, J. Dinnes, Y. Takwoingi, C. Davenport, M. Leeflang, R. Spijker, L. Hooft, D. Emperador, J. Domen, S. Horn, A. Van den Bruel, Signs and symptoms to determine if a patient presenting in primary care or hospital outpatient settings has covid-19, Cochrane Database Syst. Rev. 5 (2022), https://doi.org/10.1002/14651858.CD013665.pub2.

[2] S. Platto, Y. Wang, J. Zhou, E. Carafoli, History of the COVID-19 pandemic: origin, explosion, worldwide spreading, Biochem. Biophys. Res. Commun. 538 (2021) 14–23, https://doi.org/10.1016/j.bbrc.2020.10.087.

[3] R.C. Khanna, M.V. Cicinelli, S.S. Gilbert, S.G. Honavar, G.S.V. Murthy, COVID-19 pandemic: lessons learned and future directions, Indian J. Ophthalmol. 68 (5) (2020) 703–710, https://doi.org/10.4103/ijo.IJO_843_20.

[4] E.M. Edrada, E.B. Lopez, J.B. Villarama, E.P. Salva Villarama, B.F. Dagoc, C. Smith, A.R. Sayo, J.A. Verona, J. Trifalgar-Arches, J. Lazaro, E.G.M. Balinas, E.F.O. Telan, L. Roy, M. Galon, C.H.N. Florida, T. Ukawa, A.M.G. Villanueva, N. Saito, J.R. Nepomuceno, K. Ariyoshi, C. Carlos, A.D. Nicolasora, R.M. Solante, First COVID-19 infections in the Philippines: a case report, Trop. Med. Int. Health 48 (1) (2020) 21, https://doi.org/10.1186/s41182-020-00203-0.

[5] O.G.V. Ubaldo, J.E.M. Palo, J.E.L. Cinco, COVID-19: a single-center ICU experience of the first wave in the Philippines, Crit. Care Res. Pract. 2021 (2021) 7510306, https://doi.org/10.1155/2021/7510306.

[6] Philippine IATF, Omnibus Guidelines on the Implementation of Community Quarantine in the Philippines, https://boi.gov.ph/wp-content/uploads/2021/05/Omnibus-Guidelines-re-Implementation-of-Community-Quarantine-in-the-Philippines-ao-May-06-2021.pdf, 2020.

[7] L.S. Estadilla, Community quarantine in the Philippines, Eubios J. Asian Int. Bioeth. 30 (5) (2020) 254–255, https://www.eubios.info/EJAIB62020.pdf.

[8] B.M. Vallejo, R.A.C. Ong, Policy responses and government science advice for the COVID 19 pandemic in the Philippines: January to April 2020, Prog. Disaster Sci. 7 (2020) 100115, https://doi.org/10.1016/j.pdisas.2020.100115.

[9] Department of Health, DOH Reports 1 COVID Death and 3 New Cases, https://doh.gov.ph/doh-press-release/DOH-REPORTS-1-COVID-DEATH-AND-3-NEW-CASES, 2020.

[10] A. Raghavan, M.A. Demircioglu, S. Orazgaliyev, COVID-19 and the new normal of organizations and employees: an overview, Sustainability 13 (21) (2021) 11942, https://doi.org/10.3390/su132111942.

[11] D.A.S. Talabis, A.L. Babierra, C.A.H. Buhat, D.S. Lutero, K.M. Quindala, J.F. Rabajante, Local government responses for COVID-19 management in the Philippines, BMC Public Health 21 (1) (2021) 1711, https://doi.org/10.1186/s12889-021-11746-0.

[12] A. Gupta, S. Banerjee, S. Das, Significance of geographical factors to the COVID-19 outbreak in India, Model. Earth Syst. Environ. 6 (2020) 2645–2653, https://doi.org/10.1007/s40808-020-00838-2.

[13] D. Phiri, S. Salekin, V.R. Nyirenda, M. Simwanda, M. Ranagalage, Y. Murayama, Spread of COVID-19 in Zambia: an assessment of environmental and socioeconomic factors using a classification tree approach, Sci. Afr. 12 (2021) e00827, https://doi.org/10.1016/j.sciaf.2021.e00827.

[14] A. Mollalo, B. Vahedi, K.M. Rivera, GIS-based spatial modeling of COVID-19 incidence rate in the continental United States, Sci. Total Environ. 728 (2020) 138884, https://doi.org/10.1016/j.scitotenv.2020.138884.

[15] S. Hsiang, D. Allen, S. Annan-Phan, K. Bell, I. Bolliger, T. Chong, H. Druckenmiller, L.Y. Huang, A. Hultgren, E. Krasovich, et al., The effect of large-scale anti-contagion policies on the COVID-19 pandemic, Nature 584 (2020) 262–267, https://doi.org/10.1038/s41586-020-2404-8.

[16] R.N. Thompson, Epidemiological models are important tools for guiding COVID-19 interventions, BMC Med. 18 (2020) 152, https://doi.org/10.1186/s12916-020-01628-4.

[17] I. Cooper, A. Mondal, C.G. Antonopoulos, A SIR model assumption for the spread of COVID-19 in different communities, Chaos Solitons Fractals 139 (2020) 110057, https://doi.org/10.1016/j.chaos.2020.110057.

[18] S. Mwalili, M. Kimathi, V. Ojiambo, D. Gathungu, R. Mbogo, SEIR model for COVID-19 dynamics incorporating the environment and social distancing, BMC Res. Notes 13 (2020) 352, https://doi.org/10.1186/s13104-020-05192-1.

[19] L. Wang, T. Xu, T. Stoecker, H. Stoecker, Y. Jiang, K. Zhou, Machine learning spatio-temporal epidemiological model to evaluate Germany-county-level COVID-19 risk, Mach. Learn.: Sci. Technol. 2 (3) (2021) 035031, https://doi.org/10.1088/2632-2153/ac0314.

[20] A. d'Onofrio, M. Iannelli, G. Marinoschi, P. Manfredi, Multiple pandemic waves vs multi-period/multi-phasic epidemics: global shape of the COVID-19 pandemic, J. Theor. Biol. 593 (2024) 111881, https://doi.org/10.1016/j.jtbi.2024.111881.

[21] S. Kim, A. Abdulali, S. Lee, Heterogeneity is a key factor describing the initial outbreak of COVID-19, Appl. Math. Model. 117 (2023) 714–725, https://doi.org/10.1016/j.apm.2023.01.005.

[22] A.R.S. Castañeda, E.E. Ramirez-Torres, L.E. Valdés-García, H.M. Morandeira-Padrón, D.S. Yanez, J.I. Montijano, L.E.B. Cabrales, Modified SEIR epidemic model including asymptomatic and hospitalized cases with correct demographic evolution, Appl. Math. Comput. 456 (2023) 128122, https://doi.org/10.1016/j.amc.2023.128122.

[23] J.P. Tripathi, N. Kumawat, K. Tanwar, D. Palla, M. Martcheva, Transmission dynamics of COVID-19 with diabetes in India: a cost-effective and optimal control analysis, J. Biol. Syst. 32 (02) (2024) 643–681, https://doi.org/10.1142/S0218339024500232.

[24] S. Bugalia, J.P. Tripathi, H. Wang, Mathematical modeling of intervention and low medical resource availability with delays: applications to COVID-19 outbreaks in Spain and Italy, Math. Biosci. Eng. 18 (5) (2021) 5865–5920, https://doi.org/10.3934/mbe.2021295.

[25] A. Antelmi, G. Cordasco, V. Scarano, C. Spagnuolo, Modeling and evaluating epidemic control strategies with high-order temporal networks, IEEE Access 9 (2021) 140938–140964, https://doi.org/10.1109/ACCESS.2021.3119459.

[26] W. Wang, Y. Nie, W. Li, T. Lin, M.-S. Shang, S. Su, Y. Tang, Y.-C. Zhang, G.-Q. Sun, Epidemic spreading on higher-order networks, Phys. Rep. 1056 (2024) 1–70, https://doi.org/10.1016/j.physrep.2024.01.003.

[27] N. Kumawat, M. Rashid, A. Srivastava, J.P. Tripathi, Hysteresis and Hopf bifurcation: deciphering the dynamics of an in-host model of SARS-CoV-2 with logistic target cell growth and sigmoidal immune response, Chaos Solitons Fractals 176 (2023) 114151, https://doi.org/10.1016/j.chaos.2023.114151.

[28] Y. Bali, V.P. Bajiya, J.P. Tripathi, A. Mubayi, Exploring data sources and mathematical approaches for estimating human mobility rates and implications for understanding COVID-19 dynamics: a systematic literature review, J. Math. Biol. 88 (67) (2024) 1–39, https://doi.org/10.1007/s00285-024-02082-z.

[29] S. Bugalia, J.P. Tripathi, H. Wang, Estimating the time-dependent effective reproduction number and vaccination rate for COVID-19 in the USA and India, Math. Biosci. Eng. 20 (3) (2023) 4673–4689, https://doi.org/10.3934/mbe.2023216.

[30] A. Paul, S. Reja, S. Kundu, S. Bhattacharya, COVID-19 pandemic models revisited with a new proposal: plenty of epidemiological models outcast the simple population dynamics solution, Chaos Solitons Fractals 144 (2021) 110697, https://doi.org/10.1016/j.chaos.2021.110697.

[31] N.J.L. Haw, J. Uy, K.T.L. Sy, M.R.M. Abrigo, Epidemiological profile and transmission dynamics of COVID-19 in the Philippines, Epidemiol. Infect. 148 (2020) e204, https://doi.org/10.1017/S0950268820002137.

[32] J.M. Caldwell, E. de Lara-Tuprio, T.R. Teng, M.R.J.E. Estuar, R.F.R. Sarmiento, M. Abayawardana, R.N.F. Leong, R.T. Gray, J.G. Wood, L.-V. Le, E.S. McBryde, R. Ragonnet, J.M. Trauer, Understanding COVID-19 dynamics and the effects of interventions in the Philippines: a mathematical modelling study, Lancet Reg. Health West. Pac. 14 (2021) 100211, https://doi.org/10.1016/j.lanwpc.2021.100211.

[33] Philippine Statistics Authority, Highlights of the National Capital Region (NCR) Population - 2020 census of population and housing, https://rssoncr.psa.gov.ph/content/RSSO/highlights-national-capital-region-ncr-population-2020-census-population-and-housing-2020. (Accessed 20 January 2024).

[34] National Statistical Coordination Board, PSGC Interactive, https://web.archive.org/web/20130117174855/http://nscb.gov.ph/activestats/psgc/listcity.asp, 2012. (Accessed 20 January 2024).

[35] COVID-19 Dashboard, https://www.covid19.gov.ph/security/timeline-events/COVID_19_RESPONSE. (Accessed 20 January 2024).

[36] L.E. Añonuevo, Z.P.T. Lachica, D.A. Amistas, J.I.E. Lato, H.L.C. Bontilao, J.M.G. Catalan, R.J.F. Pasion, A.P. Yumang, A.E.S. Almocera, J.P. Arcede, et al., Transmission dynamics and baseline epidemiological parameter estimates of Coronavirus disease 2019 pre-vaccination: Davao City, Philippines, PLoS ONE 18 (4) (2023) e0283068, https://doi.org/10.1371/journal.pone.0283068.
[37] Baguio City Public Information Office, PIO Baguio, Advisory on strict border control, reversion to twice-a-week mall and market schedule and reimplementation of general lockdown on Sundays, https://web.facebook.com/pio.baguio/photos/603065593678900, 2020. (Accessed 15 February 2021).
[38] Baguio City Public Information Office, PIO Baguio, New market schedule, mall and market schedule passes are only applicable at the Baguio public market and will not be required in entering malls and other private establishments, https://web.facebook.com/pio.baguio/photos/625871914731601, 2020. (Accessed 15 February 2021).
[39] Baguio City Public Information Office, PIO Baguio, Night market reopening, https://web.facebook.com/pio.baguio/photos/690490558269736, 2020. (Accessed 15 February 2021).
[40] Baguio City Public Information Office, PIO Baguio, Reopening of city's tourism, https://web.facebook.com/pio.baguio/photos/645887749396684, 2020. (Accessed 15 February 2021).
[41] Baguio City Public Information Office, PIO Baguio, Revising portions of the general guidelines for the city of Baguio while it is under mgcq, https://web.facebook.com/pio.baguio/photos/662753041043488, 2020. (Accessed 15 February 2021).
[42] A. Canabarro, E. Tenório, R. Martins, L. Martins, S. Brito, R. Chaves, Data-driven study of the COVID-19 pandemic via age-structured modelling and prediction of the health system failure in Brazil amid diverse intervention strategies, PLoS ONE 15 (7) (2020) e0236310, https://doi.org/10.1371/journal.pone.0236310.
[43] O. Diekmann, J.A.P. Heesterbeek, J.A.J. Metz, On the definition and the computation of the basic reproduction ratio R_0 in models for infectious diseases in heterogeneous populations, J. Math. Biol. 28 (1990) 365–382, https://doi.org/10.1007/BF00178324.
[44] A. Cori, S. Cauchemez, N.M. Ferguson, C. Fraser, E. Dahlqwist, P.A. Demarsh, T. Jombart, Z.N. Kamvar, J. Lessler, S. Li, J.A. Polonsky, J. Stockwin, R. Thompson, R. van Gaalen, EpiEstim: estimate time varying reproduction numbers from epidemic curves, https://cran.r-project.org/web/packages/EpiEstim/index.html, 2021.
[45] Department of Health, D.O.H, COVID-19 Tracker Philippines, https://doh.gov.ph/covid19tracker, 2023. (Accessed 21 August 2023).
[46] H.T. Banks, S. Hu, W.C. Thompson, Modeling and Inverse Problems in the Presence of Uncertainty, CRC Press, 2014.
[47] W.L. Hallauer Jr., W.C. Slemp, R.K. Kapania, MATLAB® curve-fitting for estimation of structural dynamic parameters, 2007.
[48] M. Chinazzi, J.T. Davis, M. Ajelli, C. Gioannini, M. Litvinova, S. Merler, A.P.Y. Piontti, K. Mu, L. Rossi, K. Sun, C. Viboud, X. Xiong, H. Yu, M.E. Halloran, I.M. Longini, A. Vespignani, The effect of travel restrictions on the spread of the 2019 novel coronavirus (COVID-19) outbreak, Science 368 (2020) 395–400, https://doi.org/10.1126/science.aba9757.
[49] E. Pepe, P. Bajardi, L. Gauvin, F. Privitera, B. Lake, C. Cattuto, M. Tizzoni, COVID-19 outbreak response, a dataset to assess mobility changes in Italy following national lockdown, Sci. Data 7 (2020) 230, https://doi.org/10.1038/s41597-020-00575-2.
[50] Y. Li, R. Zhang, J. Zhao, M.J. Molina, Understanding transmission and intervention for the COVID-19 pandemic in the United States, Sci. Total Environ. 748 (2020) 141560, https://doi.org/10.1016/j.scitotenv.2020.141560.
[51] P. Gautam Jamdade, S. Gautamrao Jamdade, Modeling and prediction of COVID-19 spread in the Philippines by October 13, 2020, by using the VARMAX time series method with preventive measures, Results Phys. 20 (2021) 103694, https://doi.org/10.1016/j.rinp.2020.103694.
[52] E. de Lara-Tuprio, C.D.S. Estadilla, J.M.R. Macalalag, T.R. Teng, J. Uyheng, K.E. Espina, C.E. Pulmano, M.R.J.E. Estuar, R.F.R. Sarmiento, Policy-driven mathematical modeling for COVID-19 pandemic response in the Philippines, Epidemics 40 (2022) 100599, https://doi.org/10.1016/j.epidem.2022.100599.